Featured Article

Impaired Folding of the Mitochondrial Small TIM Chaperones Induces Clearance by the *i*-AAA Protease

Michael J. Baker[1,2], Ved P. Mooga[1], Bernard Guiard[3], Thomas Langer[2], Michael T. Ryan[1] and Diana Stojanovski[1]

1 - Department of Biochemistry, *La Trobe Institute for Molecular Science and ARC Centre of Excellence for Coherent X-ray Science, La Trobe University, Melbourne 3086, Australia*
2 - Institute for Genetics, *University of Cologne, Cologne 50674, Germany*
3 - Centre de Génétique Moléculaire, *CNRS, 91190 Gif-sur-Yvette, France*

Correspondence to Michael T. Ryan and Diana Stojanovski: *M.Ryan@latrobe.edu.au; D.Stojanovski@latrobe.edu.au*
http://dx.doi.org/10.1016/j.jmb.2012.09.019
Edited by M. Gottesman

Abstract

The intermembrane space of mitochondria contains a dedicated chaperone network—the small translocase of the inner membrane (TIM) family—for the sorting of hydrophobic precursors. All small TIMs are defined by the presence of a twin CX_3C motif and the monomeric proteins are stabilized by two intramolecular disulfide bonds formed between the cysteines of these motifs. The conserved cysteine residues within small TIM members have also been shown to participate in early biogenesis events, with the most N-terminal cysteine residue important for import and retention within the intermembrane space via the receptor and disulfide oxidase, Mia40. In this study, we have analyzed the *in vivo* consequences of improper folding of small TIM chaperones by generating site-specific cysteine mutants and assessed the fate of the incompletely oxidized proteins within mitochondria. We show that no individual cysteine residue is required for the function of Tim9 or Tim10 in yeast and that defective assembly of the small TIMs induces their proteolytic clearance from mitochondria. We delineate a clearance mechanism for the mutant proteins and their unassembled wild-type partner protein by the mitochondrial ATP-dependent protease, Yme1 (yeast mitochondrial escape 1).

Introduction

In the yeast *Saccharomyces cerevisiae*, ~1000 precursor proteins need to be imported into mitochondria and subsequently sorted to the correct mitochondrial subcompartment: the outer membrane, intermembrane space (IMS), inner membrane, and matrix.[1–4] A family of small translocase of the inner membrane (TIM) chaperones resides in the IMS of mitochondria and sort hydrophobic precursors of the outer membrane β-barrel family and inner membrane carrier family through this aqueous compartment.[2,3,5–7] In yeast, there are five small TIM members—Tim8, Tim9, Tim10, Tim12, and Tim13.[7] Tim9 partners with Tim10, while Tim13 partners with Tim8 to form soluble hexameric chaperone complexes.[8–10] Tim12 is found exclusively at the inner membrane carrier translocase (TIM22 complex),[11,12] a machinery dedicated to the biogenesis of inner membrane carrier proteins. All small TIM proteins contain a twin CX_3C motif in which two cysteine residues are separated by three amino acid residues.[7] Despite initial controversy, structural determination verified that these cysteine residues form two intramolecular disulfide bonds.[8–10,13] Each monomer is composed of a helix–loop–helix with the dual disulfides bracing the central loop structure. Monomers assemble with alternating subunits into the hexameric structure with the helices involved in substrate contacts.[8–10,13]

Like most mitochondrial proteins, the small TIMs need to be imported into mitochondria following their synthesis in the cytosol. The import of cysteine-rich IMS proteins is tightly coupled to their oxidation.[5,14–16] IMS precursors translocate

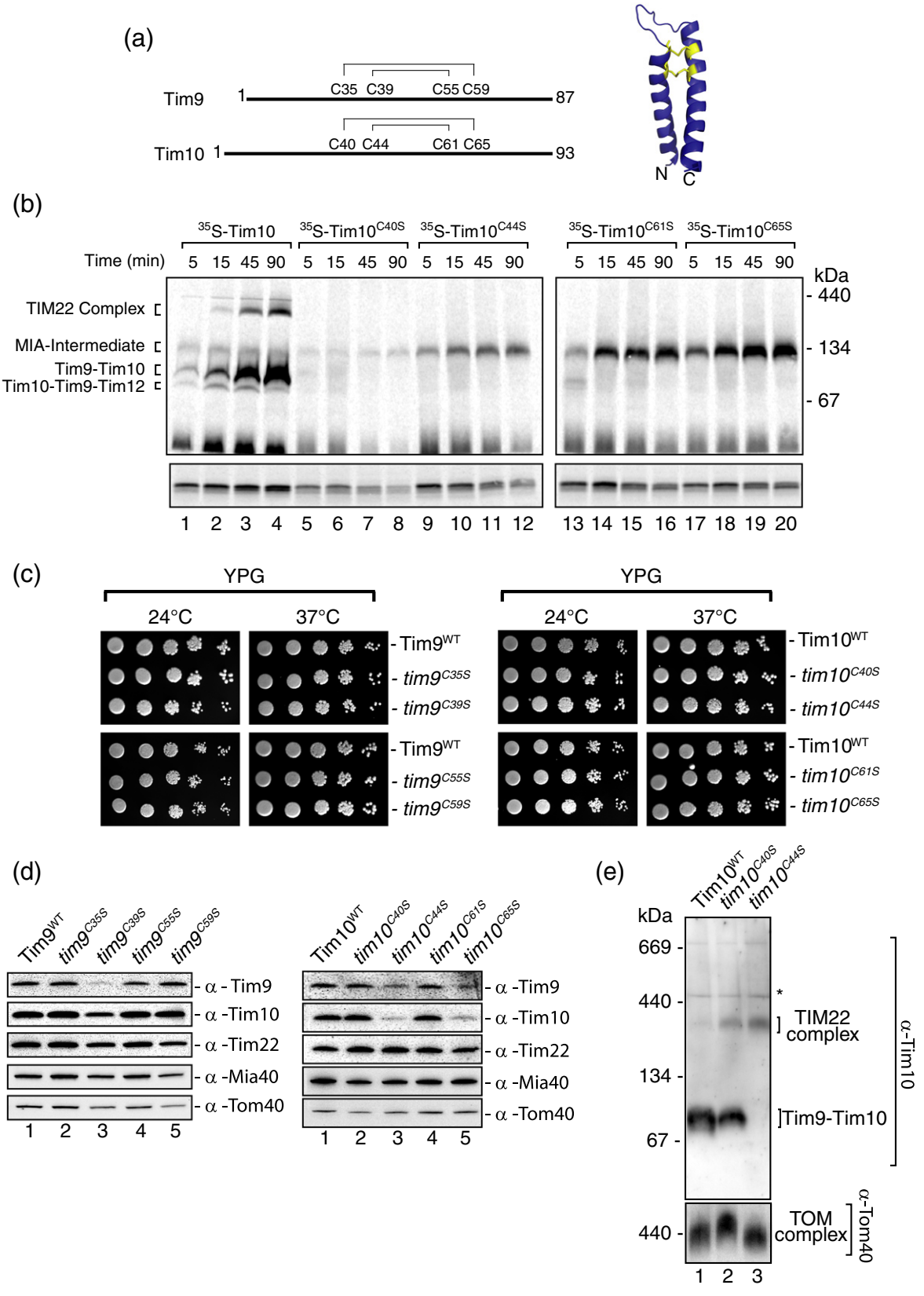

Fig. 1 (*legend on next page*)

the outer membrane through the translocase of the outer membrane (TOM) complex and use a specific redox-driven machinery within the IMS for import and assembly known as MIA (mitochondrial IMS import and assembly machinery).[2,14,15] The IMS receptor Mia40 engages incoming precursors via a transient disulfide bond and, with the help of the sulfhydryl oxidase Erv1, promotes oxidation and folding of the incoming protein.[17–19] Once oxidized, the small TIM monomers then form the hexameric chaperone complexes.

Characterization of small TIM proteins biogenesis has been largely performed using *in vitro* assays with isolated mitochondria. Such studies revealed that the individual cysteine residues in Tim9 and Tim10 play an important role in the import and subsequent assembly of these proteins.[20,21] Specifically, the most N-terminal cysteine was found to mediate binding of the incoming small TIM precursor to Mia40, trapping it in the IMS. All cysteine residues were found to be required for complete oxidation of the proteins, allowing their subsequent assembly.[20,21] However, studies utilizing *in vivo* models to elucidate the mechanisms that contribute to substrate oxidation in the IMS are lacking. Furthermore, our understanding of the mechanisms that come into play when IMS precursors are improperly oxidized or folded remains limited. In an effort to expand our understanding on the oxidation and folding requirements for IMS proteins in a cellular context, we assessed the importance of small TIM cysteine residues *in vivo*. We show that no individual cysteine residue within Tim9 and Tim10 is essential for yeast viability and the presence of a single disulfide bond in either Tim9 or Tim10 is sufficient for yeast survival. However, the incompletely oxidized proteins are present in mitochondria at reduced levels, and this correlates with a reduction in the steady-state levels of the corresponding wild-type partner protein. We show that the improperly folded unassembled chaperones are targeted for degradation in a process that requires the mitochondrial *IMS*-AAA (*i*-AAA) protease.

Our results describe a novel clearance mechanism for improperly folded or assembled IMS proteins.

Results

No individual cysteine residue in the Tim9 and Tim10 dual CX_3C motif is required for yeast viability

The crystal structures of Tim9 and Tim10 revealed that the first and fourth, and the second and third cysteine residues form intramolecular disulfide bonds, stabilizing the monomeric subunits (Fig. 1a).[8,9] Import and assembly of Tim9 and Tim10 can be visualized using an *in vitro* assay where newly translated ^{35}S-labeled Tim9 or Tim10 is incubated with isolated mitochondria for various times and then complexes containing radiolabeled proteins are analyzed by blue native polyacrylamide gel electrophoresis (BN-PAGE). Imported ^{35}S-Tim10 shows an engagement with Mia40 at ~130 kDa (MIA intermediate), and following oxidation, it assembles into the hexameric complex with Tim9 (Tim9–Tim10) and also in an assembly intermediate with Tim12 and Tim10 (Tim10–Tim9–Tim12) before integrating into the TIM22 complex (Fig. 1b). Mutation of any cysteine residue within the dual CX_3C motif leads to apparent assembly defects with stalling at the MIA complex. Furthermore, it has been shown that the most N-terminal cysteine in Tim9 or Tim10 is required for docking onto Mia40 and preventing backsliding of the protein out of mitochondria.[20,21] While these *in vitro* results are instructive, we chose to study the consequences of introducing such mutations into Tim9 and Tim10 proteins *in vivo*, where there is a greater level of complexity.

As Tim9 and Tim10 are essential for cell viability, we employed a plasmid shuffling approach. Each cysteine residue in the CX_3C motif of Tim9 and Tim10 was mutated to serine (generating *tim9*^{C35S}, *tim9*^{C39S}, *tim9*^{C55S}, and *tim9*^{C59S}, and *tim10*^{C40S}, *tim10*^{C44S}, *tim10*^{C61S}, and *tim10*^{C65S}). Plasmids encoding the mutant proteins were transformed into the appropriate deletion strain *tim9*Δ or *tim10*Δ (carrying the wild-type genes on plasmids carrying a URA3 marker) and subjected to 5-fluoroorotic acid (5-FOA) for loss of URA3 plasmids and ultimately the

Fig. 1. Tim9 and Tim10 cysteine mutants are viable. (a) Schematic representation of Tim9 and Tim10 cysteine residues and a ribbon diagram depicting the individual Tim10 subunit. Cysteines are depicted in yellow. (b) Isolated wild-type mitochondria were incubated with equivalent amounts of ^{35}S-Tim10 and ^{35}S-Tim10 cysteine mutants. Following import, mitochondria were isolated and solubilzed in digitonin-containing buffer and analyzed by BN-PAGE. (c) Serial dilutions of yeast cells expressing wild-type or mutant Tim9 (left panel) and wild-type or mutant Tim10 (right panel) grown at 24 °C and 37 °C onto non-fermentable (glycerol) media. (d) Mitochondria isolated from wild-type and Tim9 cysteine mutants (left panel) and wild-type and Tim10 cysteine mutants (right panel) were analyzed by SDS-PAGE and immunodecoration with the indicated antibodies. (e) Mitochondria isolated from cells expressing Tim10^{WT}, Tim10^{C40S}, and Tim10^{C44S} were solubilized in digitonin-containing buffer and separated by BN-PAGE. Following electrophoresis, samples were analyzed by Western blotting using anti-Tim10 (upper panel) or anti-Tom40 (lower panel) antibodies. The asterisk indicates nonspecific species.

wild-type proteins. All of the individual cysteine mutants were able to grow on 5-FOA-containing media (data not shown), suggesting that the mutant proteins could complement the loss of wild-type Tim9 or Tim10. Cells were serially diluted and spotted onto non-fermentable media and growth was monitored at different temperatures to evaluate any growth defects as a consequence of mitochondrial dysfunction. All mutants grew as efficiently as the wild-type strain (Fig. 1c). We isolated mitochondria from wild-type and mutant strains and assessed steady-state levels of mitochondrial proteins by Western blotting (Fig. 1d). Mitochondrial marker proteins, including the small TIM substrates Tim22 and Tom40 were largely unaffected when compared to wild-type mitochondria. However, the levels of the mutant proteins Tim9^{C39S}, Tim10^{C44S}, and Tim10^{C65S} were reduced to different degrees. We addressed whether these mutants can assemble by looking at a Tim10 mutant showing low steady-state levels of Tim9 and Tim10 (Tim10^{C44S}) and one mutant that displays normal levels (Tim10^{C40S}) using BN-PAGE (Fig. 1e). Interestingly, cells expressing Tim10^{C40S} display normal levels of the Tim9–Tim10 hexamer, and this correlates with the normal steady-state levels of these proteins in the mutant (Fig. 1d, right panel). Conversely for Tim10^{C44S}, we do not see hexameric assembly, and this correlates with the reduced steady-state levels of Tim9 and Tim10 in this mutant (Fig. 1d, right panel). Interestingly, while the levels of the hexameric species varied, the assembly of the mutant proteins was retained, or possibly enriched, at the TIM22 complex (Fig. 1e). Thus, we conclude that no individual cysteine residue in either Tim9 or Tim10 is essential for yeast viability. This was surprising given that ^{35}S-Tim9^{C35S} and ^{35}S-Tim10^{C40S} displayed striking import and assembly defects when imported into isolated mitochondria *in vitro*.[20,21]

A single disulfide bond in Tim9 and Tim10 is essential for yeast survival

The viability of the individual cysteine mutants prompted us to generate double-cysteine mutants in either Tim9 or Tim10. Three mutants were generated: one that removed the outer disulfide bond (*tim9*$^{C35S/C59S}$; *tim10*$^{C40S/C65S}$), one that removed the inner disulfide bond (*tim9*$^{C39S/C55S}$; *tim10*$^{C44S/C61S}$), and a mutant that would disrupt both disulfide bonds (*tim9*$^{C35S/C55S}$; *tim10*$^{C40S/C61S}$). Yeast harboring Tim9 or Tim10 lacking both disulfide bonds were not viable (shown for Tim10, Fig. 2a), confirming the importance of the disulfide brace for the biogenesis and/or function of the proteins. However, yeast cells were viable when either the outer or the inner disulfide bond was lacking (Fig. 2b). Analysis of liquid cultures revealed a growth defect for cells expressing the inner disulfide mutants of both Tim9 and Tim10 (*tim9*$^{C39S/C55S}$ and *tim10*$^{C44S/C61S}$) at 37 °C (Fig. 2c). We isolated mitochondria from wild-type yeast and strains expressing the double-cysteine mutants, and immunoblot analysis revealed that the steady-state levels of mitochondrial marker proteins tested, including the small TIM substrates Tim22, Tom40, and ADP/ATP carrier (AAC), were not altered (Fig. 2d). However, we noticed a marked decrease in the steady-state levels of the respective mutant Tim9 and Tim10 proteins. The reduced levels may be due to defective import of the mutant or folding and assembly (or both). However, we also found that the reduced steady-state levels of the mutant proteins correlated with a reduction in the steady-state levels of the corresponding wild-type partner protein (Fig. 2d). As the wild-type proteins are not defective in import, it suggests that they are turned over by a proteolytic machinery.

Tim9–Tim10 chaperone pathways are affected in disulfide mutants

To determine if there were any functional consequences due to the presence of mutant small TIM proteins in mitochondria, we assessed the import and assembly of mitochondrial precursors. For this analysis, we selected the Tim10 double-cysteine mutants. We imported the radiolabeled matrix-targeted pSu9-DHFR (dihydrofolate reductase), which is not dependent on the small TIMs for its import and observed no defect in the mutant mitochondria (Fig. 3a). Given that pSu9-DHFR is dependent on the membrane potential ($\Delta\psi$), this result also indicates that the mitochondrial membrane potential was not significantly impaired in these mutant cells. We next looked at the model small TIM substrate, the inner membrane AAC. ^{35}S-AAC was imported into mitochondria isolated from wild-type, *tim10*$^{C40S/C65S}$, and *tim10*$^{C44S/C61S}$ mitochondria in the presence or absence of a $\Delta\psi$ (the insertion of carrier proteins into the inner membrane is a $\Delta\psi$-dependent process). Following import, we treated samples with proteinase K to remove non-imported precursors. AAC assembly can be monitored by BN-PAGE, since it assembles into a dimeric species within the inner membrane.[22] Assembly of AAC was mildly delayed in *tim10*$^{C40S/C65S}$ and blocked in *tim10*$^{C44S/C61S}$ mitochondria when compared to wild type, consistent with the growth phenotype of these mutants (Fig. 3b, upper panel). Analysis by SDS-PAGE confirmed that import of AAC into *tim10*$^{C44S/C61S}$ mitochondria was reduced (Fig. 3b, lower panel), consistent with a translocation defect due to impaired function of the Tim9–Tim10 complex.

The small TIMs are involved in distinct stages in the biogenesis of carrier proteins; they (i) ratchet the carrier precursors across the outer membrane at the TOM complex and (ii) sort the carrier precursors

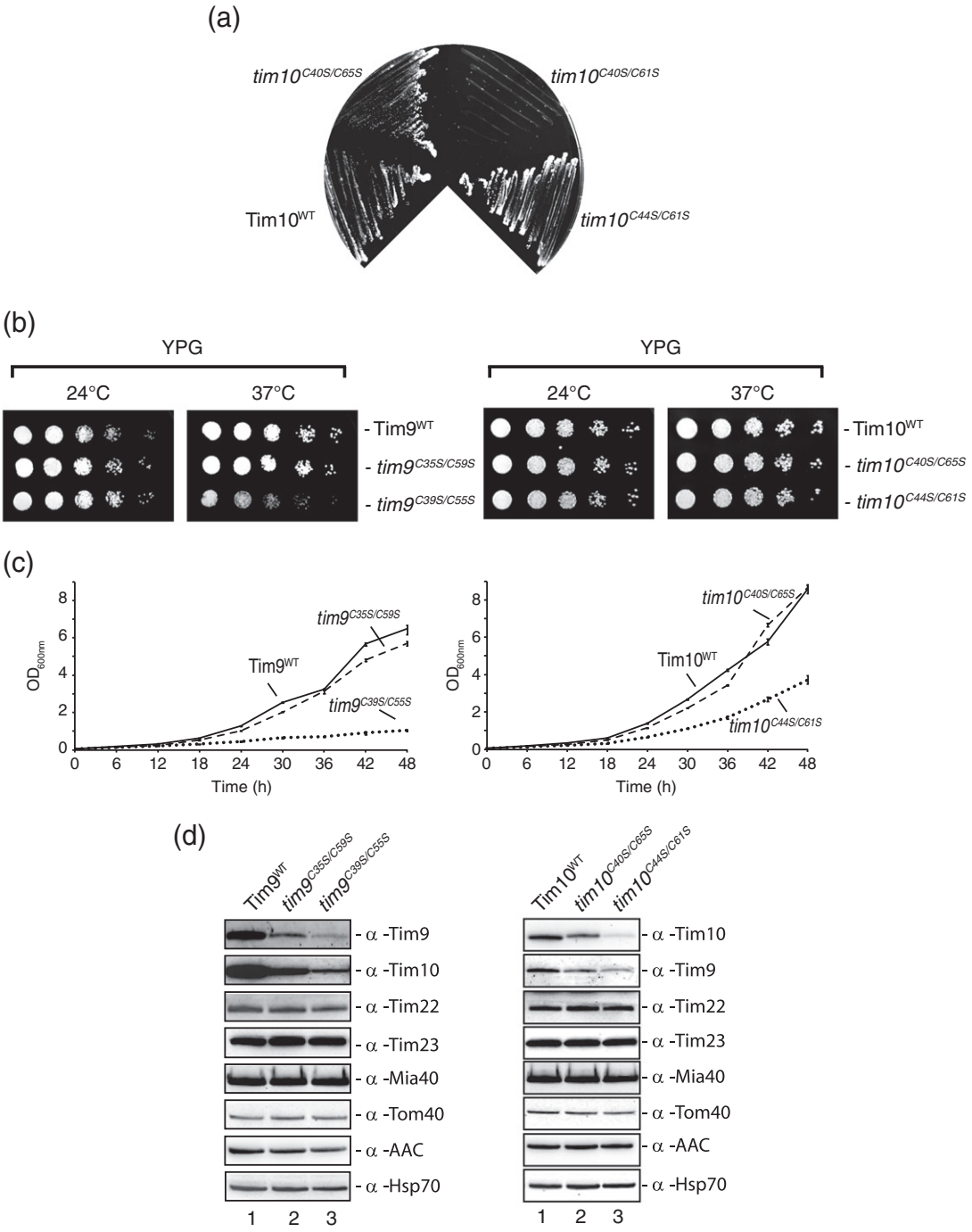

Fig. 2. Tim9 and Tim10 require a single disulfide bond to function. (a) Growth of yeast cells expressing Tim10^{WT}, *tim10*$^{C40S/C65S}$, *tim10*$^{C44S/C61S}$, and *tim10*$^{C40S/C61S}$ plated on 5-FOA and grown at 24 °C. (b) Cells expressing Tim9^{WT}, *tim9*$^{C35S/C59S}$, and *tim9*$^{C39S/C55S}$ (left panel) and Tim10^{WT}, *tim10*$^{C40S/C65S}$, and *tim10*$^{C44S/C61S}$ (right panel) were serially diluted and their growth was analyzed at 24 °C and 37 °C on non-fermentable (glycerol) media. (c) Tim9^{WT}, *tim9*$^{C35S/C59S}$, and *tim9*$^{C39S/C55S}$ (left panel) or Tim10^{WT}, *tim10*$^{C40S/C65S}$, and *tim10*$^{C44S/C61S}$ (right panel) strains were inoculated in liquid cultures to equal densities and their growth on a non-fermentable carbon source was assessed at 37 °C for 48 h. Samples were retrieved at 6-h intervals and the optical density of the culture was measured at 600 nm (error bars represent the standard error of the mean; n=3). (d) Mitochondria were isolated from strains harboring wild-type and Tim9 (left panel) and Tim10 (right panel) double-cysteine mutants. Equal amounts of proteins were separated by SDS-PAGE and analyzed with the indicated antibodies by immunodecoration.

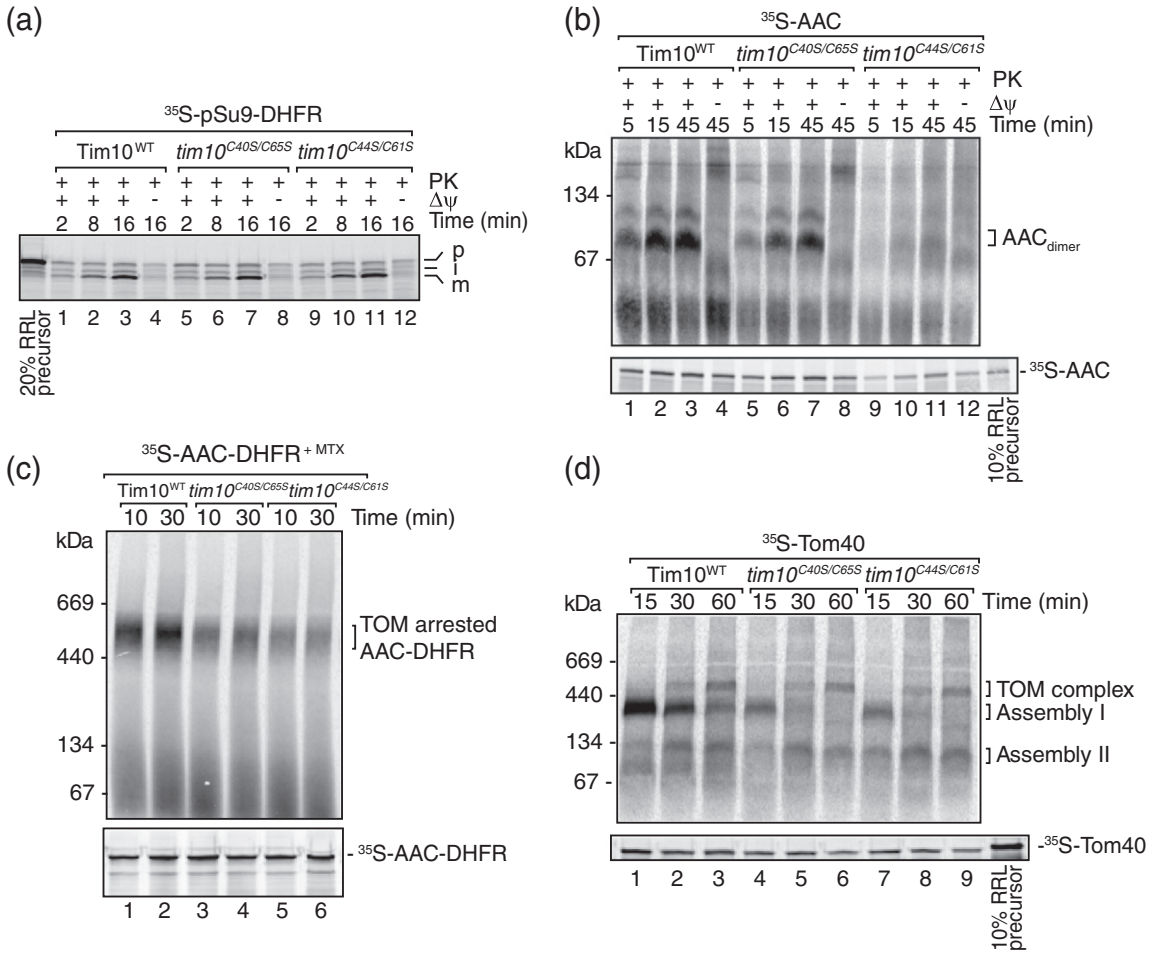

Fig. 3. Functional characterization of Tim10 double-cysteine mutants. (a) ^{35}S-pSu9-DHFR was incubated with mitochondria isolated from Tim10^{WT}, *tim10*$^{C40S/C65S}$, and *tim10*$^{C44S/C61S}$ yeast cells for increasing times at 25 °C in the presence (+) or absence (–) of a membrane potential (Δψ). Following import, samples were treated with proteinase K (PK) and subsequently analyzed by SDS-PAGE and autoradiography. Twenty percent of the input rabbit reticulocyte lysate (RRL)-containing precursor is indicated. p, precursor; i, intermediate; m, mature. (b) ^{35}S-AAC was incubated with Tim10^{WT}, *tim10*$^{C40S/C65S}$, and *tim10*$^{C44S/C61S}$ mitochondria at 30 °C in the presence (+) or absence (–) of a membrane potential (Δψ). Following import, samples were split for BN-PAGE (upper panel) and SDS-PAGE (lower panel) analysis. BN-PAGE samples were solubilized in digitonin-containing buffer and SDS-PAGE samples were solubilized in Laemmli buffer. Ten percent of the input RRL-containing precursor is indicated. (c) ^{35}S-AAC-DHFR in the presence of methotrexate (MTX) was incubated with the indicated mitochondria at 30 °C for 10 and 30 min. Following import, mitochondria were re-isolated and analyzed by either BN-PAGE (upper panel) or SDS-PAGE (lower panel). (d) ^{35}S-Tom40 was incubated with isolated mitochondria from the indicated strains for 15, 30, and 60 min at 25 °C. Mitochondria were isolated and subjected to digitonin solubilzation for BN-PAGE analysis (upper panel) or solubilized in Laemmli buffer for SDS-PAGE (lower panel). Ten percent of the input RRL-containing precursor is indicated.

through the IMS and deliver them to the TIM22 complex.[9] To decipher at which stage the Tim10 double-cysteine mutants were affected, we exploited a construct of AAC fused to DHFR, which can be arrested in the TOM complex and still make contact with the Tim9–Tim10 complex in the presence of the ligand methotrexate.[22,23] We incubated ^{35}S-AAC-DHFR with mitochondria isolated from wild-type, *tim10*$^{C40S/C65S}$, and *tim10*$^{C44S/C61S}$ mitochondria and observed reduced arrest of the precursor at the TOM complex in both *tim10*$^{C40S/C65S}$ and *tim10*$^{C44S/C61S}$ mitochondria (Fig. 3c). These findings indicate that that small TIM mutants cause a defect in the ratcheting of substrates across the outer membrane.

The small TIMs also function in the sorting of β-barrel precursors to the outer membrane.[24,25] The β-barrel import pathway involves (i) translocation across the outer membrane through the TOM complex, (ii) sorting through the IMS by the small TIMs to the outer membrane sorting and assembly machinery (SAM) complex, and (iii) membrane

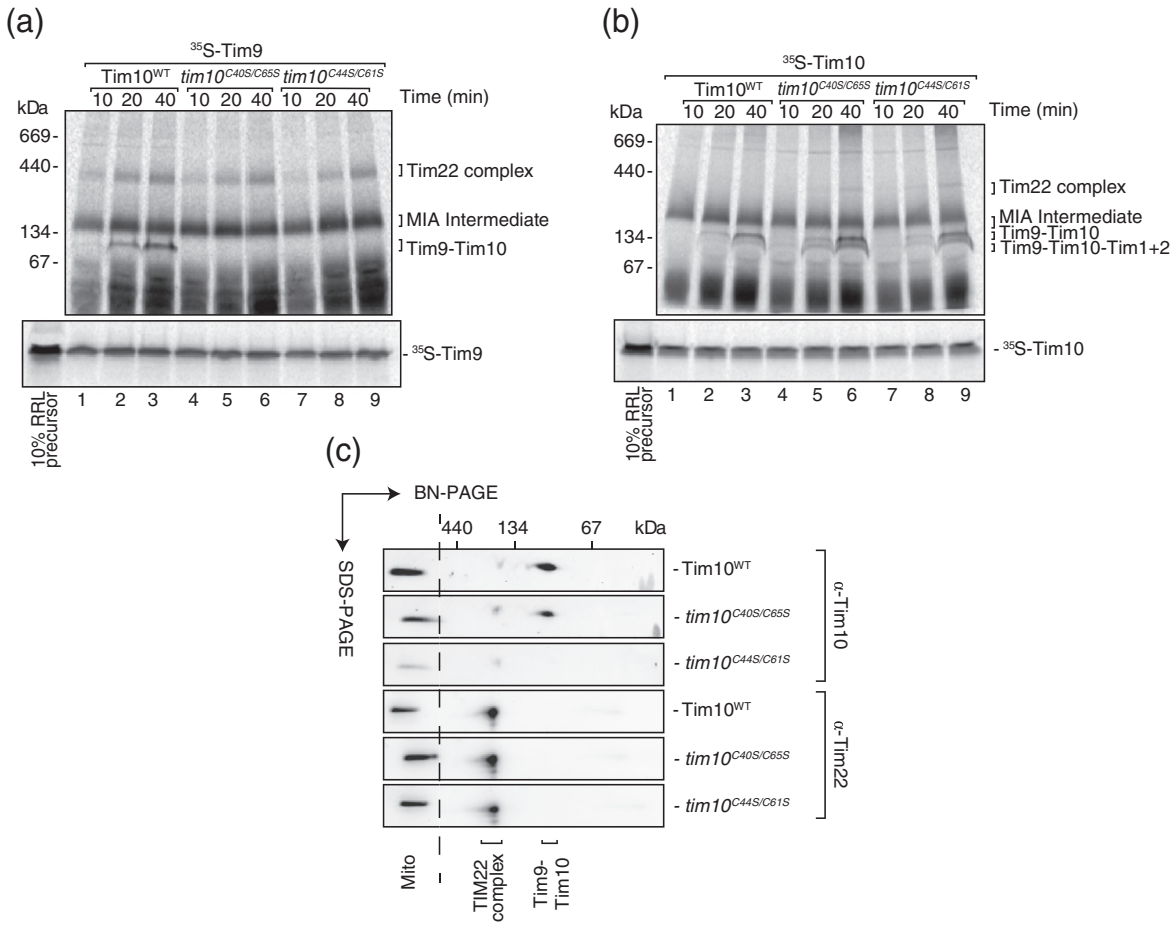

Fig. 4. (a) ^{35}S-Tim9 was incubated with Tim10^{WT}, *tim10*$^{C40S/C65S}$, and *tim10*$^{C44S/C61S}$ mitochondria at 30 °C for increasing times. Following import, samples were split for BN-PAGE (upper panel) and SDS-PAGE (lower panel). BN-PAGE samples were solubilized in digitonin and SDS-PAGE samples were solubilized in Laemmli buffer. Ten percent of the input rabbit reticulocyte lysate (RRL)-containing precursor is indicated. (b) ^{35}S-Tim10 was incubated with Tim10^{WT}, *tim10*$^{C40S/C65S}$, and *tim10*$^{C44S/C61S}$ mitochondria at 30 °C for increasing times. Following import, samples were split for BN-PAGE (upper panel) and SDS-PAGE (lower panel). BN-PAGE samples were solubilized in digitonin and SDS-PAGE samples were solubilized in Laemmli buffer. Ten percent of the input RRL-containing precursor is indicated. (c) Mitochondria isolated from Tim10^{WT}, *tim10*$^{C40S/C65S}$, and *tim10*$^{C44S/C61S}$ cells were subjected to BN-PAGE in the first dimension and SDS-PAGE in the second dimension followed by Western analysis with α-Tim10 and α-Tim22 antibodies. TIM22 complex and the Tim9–Tim10 hexamer are indicated. Mito denotes control mitochondrial sample subjected to SDS-PAGE only.

integration. The assembly pathway of the β-barrel protein Tom40 can be monitored by BN-PAGE and appears as a series of assembly intermediates, namely, association with the SAM complex (Intermediate I), integration into the membrane (Intermediate II), and final assembly into the mature TOM complex.[26,27]

When we performed import of ^{35}S-Tom40 into isolated wild-type mitochondria, all steps proceeded as expected (Fig. 3d, lanes 1–3). However, import of Tom40 into mitochondria from *tim10*$^{C40S/C65S}$ or *tim10*$^{C44S/C61S}$ cells displayed reduced accumulation of the precursor at the SAM complex (Fig. 3d, compare lanes 4 and 7 with lane 1), suggesting defects in sorting of precursors from TOM to SAM.

Since mutations in Tim10 can affect the assembly/function of either or both the Tim9–Tim10 hexamer and the TIM22 complex, we examined the assembly of the small TIM proteins themselves. ^{35}S-Tim9 and ^{35}S-Tim10 were imported into wild-type and Tim10 double-cysteine mutant mitochondria and their assembly was monitored by BN-PAGE (Fig. 4a and b). Import of ^{35}S-Tim9 revealed a productive MIA intermediate and assembly into the TIM22 complex in all mitochondrial samples (Fig. 4a). However, a lack of assembly into the soluble Tim9–Tim10 complex was apparent in mitochondria isolated

from *tim10*$^{C40S/C65S}$ and *tim10*$^{C44S/C61S}$ strains. This suggests that the mutant Tim10$^{C40S/C65S}$ or Tim10$^{C44S/C61S}$ molecules are not capable of assembling with the incoming wild-type Tim9 subunit. Conversely, imported ^{35}S-Tim10 was capable of assembling into the Tim9–Tim10 complex and the Tim9–Tim10–Tim12 assembly intermediate (Fig. 4b). These data suggested a potential defect in the generation of the soluble Tim9–Tim10 hexamer; therefore, we examined the steady-state levels of hexameric complex in Tim10 mutant mitochondria by BN-PAGE followed by SDS-PAGE in the second dimension (Fig. 4c). Western analysis with Tim22 antibodies confirmed that the TIM22 complex was intact in mutant and wild-type mitochondria (Fig. 4c, lower panels, α-Tim22). Probing with Tim10 antibodies revealed that Tim10$^{C40S/C65S}$ and Tim10$^{C44S/C61S}$ were also present at comparable levels within the TIM22 complex. However, the hexameric Tim9–Tim10 complex was reduced for Tim10$^{C40S/C65S}$ relative to wild-type mitochondria or completely absent for Tim10$^{C44S/C61S}$ (Fig. 4c, upper panels, α-Tim10). We conclude that the Tim10 double-cysteine mutants have defects in their biogenesis and specific assembly into the soluble Tim9–Tim10 hexamer, providing an explanation for the observed growth and import defects in these strains.

Mutant small TIMs and their hexameric partners are turned over by the *i*-AAA protease Yme1

The reduced levels of the cysteine mutants within mitochondria and their respective partner proteins (Figs. 2d and 4c) provided us with a tool to explore the fate of improperly folded and assembled IMS substrates *in vivo*. We reasoned that the reduced steady-state levels of the small TIMs could be due to either a defect in their import into mitochondria or regulated proteolytic turnover within mitochondria due to folding/assembly defects. However, given that the mutant precursors can form productive intermediates with Mia40 and can reach mitochondria (Fig. 1b), we reasoned that it is unlikely to be an import defect.[20,21] Therefore, we postulated that the incomplete oxidation renders the proteins unstable,

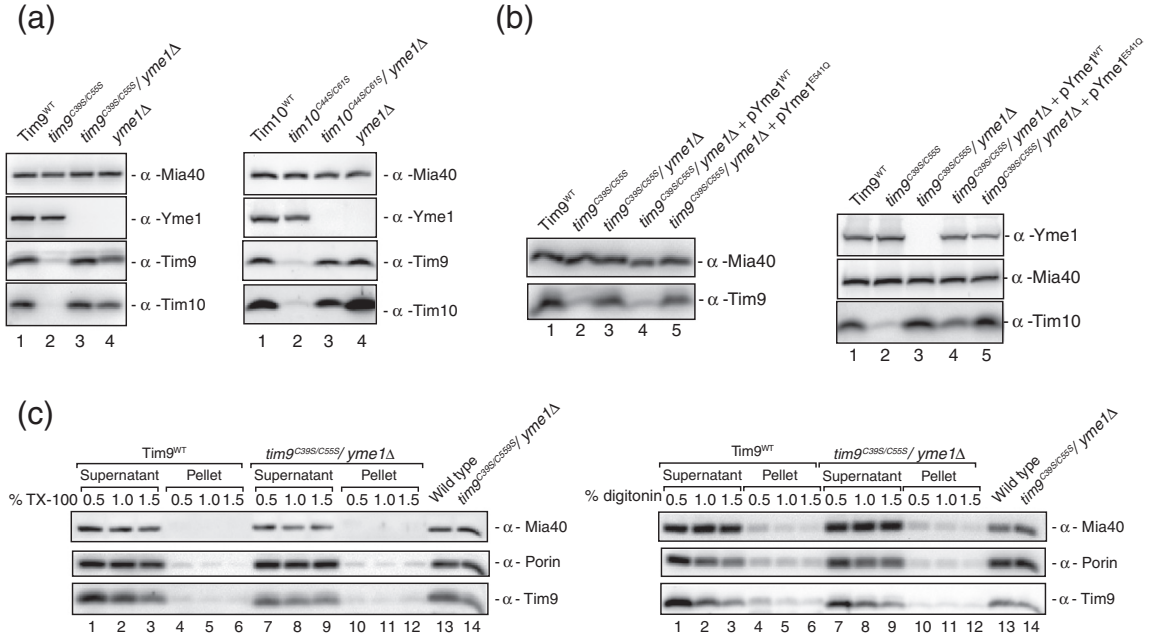

Fig. 5. Proteolytic regulation of misfolded and unassembled small TIMs by Yme1. (a) Mitochondria isolated from wild type (Tim9^{WT}), *tim9*$^{C39S/C55S}$, *tim9*$^{C39S/C55S}$/*yme1*Δ, and *yme1*Δ (left panel) and wild type (Tim10^{WT}), *tim10*$^{C44S/C61S}$, *tim10*$^{C44S/C61S}$/*yme1*Δ, and *yme1*Δ (right panel) were separated by SDS-PAGE and analyzed by immunoblotting using the indicated antibodies. (b) Whole-cell protein extracts were prepared from wild type (Tim9^{WT}), *tim9*$^{C39S/C55S}$, *tim9*$^{C39S/C55S}$/*yme1*Δ, *tim9*$^{C39S/C55S}$/*yme1*Δ+pYme1^{WT}, and *tim9*$^{C39S/C55S}$/*yme1*Δ+pYme1^{E541Q} yeast cells and separated by SDS-PAGE. Immunodecoration was performed with anti-Tim9 (left panel) and anti-Tim10 (right panel) antibodies and Mia40 as a loading control. Immunodecoration with Yme1 antibodies confirmed the presence of the deletion in *tim9*$^{C39S/C55S}$/*yme1*Δ (lane 3) and the reintroduction of wild-type Yme1 and Yme1^{E541Q} in the *tim9*$^{C39S/C55S}$/*yme1*Δ (lanes 4 and 5). (c) Isolated mitochondria from wild type (Tim9^{WT}) and *tim9*$^{C39S/C55S}$/*yme1*Δ cells were solubilized in buffer containing Triton X-100 (left panel) or digitonin (right panel) for 30 min on ice. Samples were clarified by centrifugation and the separated soluble (supernatant) and insoluble (pellet) fractions were precipitated with TCA and analyzed by SDS-PAGE and immunoblotting with the indicated antibodies. Total mitochondrial protein levels prior to solubilization are shown in lanes 13 (wild type) and 14 (*tim9*$^{C39S/C55S}$/*yme1*Δ).

preventing their proper folding and ability to assemble with their partner subunit. This targets both the mutant and wild-type subunits for proteolytic turnover within mitochondria.

Mitochondria possess a proteolytic system that surveys protein quality control within the organelle.[28] The inner membrane of mitochondria harbors two AAA (ATPases associated with diverse cellular activities) proteases: the *matrix*-AAA and *i*-AAA proteases, which have their enzymatic and active sites localized within the matrix and IMS, respectively.[29–31] We decided to test if the *i*-AAA protease, which in yeast is composed of Yme1 (yeast mitochondrial escape 1) subunits, is involved in the turnover of the mutant small TIM proteins. We deleted *YME1* in cells expressing *tim9*$^{C39S/C55S}$ or *tim10*$^{C44S/C61S}$ and observed restored levels of mutant Tim9 or Tim10 and wild-type Tim10 and Tim9, respectively, in the absence of Yme1 (Fig. 5a; left and right panels, compare lanes 2 and 3). We performed further analysis using the *tim9*$^{C39S/C55S}$/*yme1*Δ strain and could show that the reintroduction of wild-type Yme1 into *tim9*$^{C39S/C55S}$/*yme1*Δ reduced the levels of the mutant Tim9 (Fig. 5b, left panel) and wild-type Tim10 (Fig. 5b, right panel). It has been reported that the *i*-AAA protease can contribute to protein homeostasis within mitochondria through proteostasis and also chaperone-like activity.[32] To confirm the exact role of Yme1 in the regulation of the mutant small TIM proteins, we utilized a Yme1 mutant, Yme1^{E541Q}, which harbors a mutation within its catalytic domain, thus rendering the proteolytic function inactive. Upon expression of Yme1^{E541Q} in the *tim9*$^{C39S/C55S}$/*yme1*Δ background, we observed stabilization of Tim9$^{C39S/C55S}$ (Fig. 5b, left panel, lane 5) and wild-type Tim10 (Fig. 5b, right panel, lane 5), confirming that a catalytically active Yme1 is required for the degradation of mutant small TIMs.

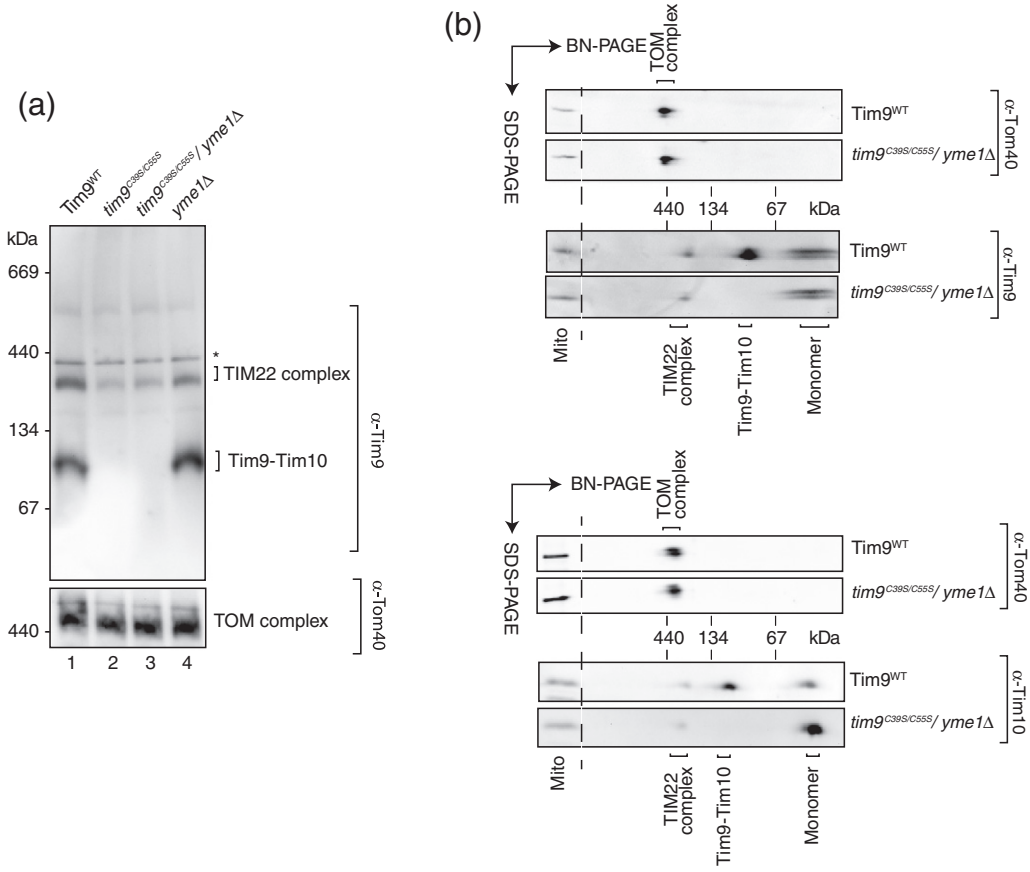

Fig. 6. Assembly of small TIM mutants in the absence of Yme1. (a) Complexes from mitochondria isolated from wild type (Tim9^{WT}), *tim9*$^{C39S/C55S}$, *tim9*$^{C39S/C55S}$/*yme1*Δ, and *yme1*Δ were solubilized in digitonin-containing buffer and separated by BN-PAGE and analyzed by immunoblotting using anti-Tim9 antibodies (upper panel) and anti-Tom40 (lower panel) as a loading control. The asterisk indicates cross-reactive species. (b) Wild type (Tim9^{WT}) and *tim9*$^{C39S/C55S}$/*yme1*Δ mitochondria were separated by BN-PAGE in the first dimension and followed by SDS-PAGE in the second dimension. Samples were analyzed by Western blotting using anti-Tom40 and anti-Tim9 antibodies (upper panel) or anti-Tom40 and anti-Tim9 antibodies (lower panel). TIM22 complex and the Tim9–Tim10 hexamer are indicated. Mito denotes control mitochondrial sample subjected to SDS-PAGE only.

To determine if the small TIMs are prone to aggregation in the absence of Yme1, we performed detergent solubility assays. Mitochondria isolated from wild-type and *tim9*$^{C39S/C55S}$/*yme1*Δ cells were solubilized in either Triton X-100 (Fig. 5c, left panel) or digitonin (Fig. 5c, right panel), and the soluble (supernatant) and insoluble (pellet) fractions were analyzed by SDS-PAGE and Western blotting. Tim9$^{C39S/C55S}$ was present in the detergent-soluble fractions, along with the marker proteins Mia40 and porin, indicating that the mutant protein does not aggregate in the absence of Yme1. Having confirmed that the reestablished Tim9$^{C39S/C55S}$ was not prone to aggregation in the absence of Yme1, we looked for the appearance of a Tim9$^{C39S/C55S}$–Tim10 hexamer in these mitochondria by BN-PAGE. However, the reestablished mutant protein was not competent for assembly with wild-type Tim10 (Fig. 6a). Using BN-PAGE followed by SDS-PAGE in the second dimension also revealed that the mutant Tim9$^{C39S/C55S}$ was not competent for assembly with wild-type Tim10, but rather that both Tim9 (Fig. 6b, upper panel) and Tim10 (Fig. 6b, lower panel) were stabilized as monomeric units in the absence of Yme1. We conclude that the presence of only a single disulfide in Tim9 renders the protein unstable and targets it, and its unassembled wild-type partner subunit, for degradation by a mitochondrial clearance system involving the *i*-AAA protease.

Discussion

Disulfide bond formation in mitochondria has been studied intensely in recent years and is linked to the Mia40-dependent oxidative folding pathway of the IMS. However, many studies of the MIA pathway have exploited *in vitro* systems, and thus, *in vivo* correlations of many of these findings have been lacking. Additionally, we have limited information on what takes place when there are glitches in the system leading to improperly oxidized and misfolded protein species within the IMS. By generating a series of cysteine mutants of the classical MIA substrates, the small TIM proteins, we have been able to explore this premise. Although we found that only a single disulfide bond in Tim9 or Tim10 is required for yeast cell viability, we did observe a growth defect for cells lacking the inner disulfide bond (*tim9*$^{C39S/C55S}$; *tim10*$^{C44S/C61S}$).

The inner disulfide mutants displayed severely reduced levels of the Tim9–Tim10 hexameric assembly *in vivo*. This observation correlates with *in vitro* data suggesting that the inner disulfide bond has an important role in the stability of the Tim9–Tim10 hexamer,[21] while work with recombinant cysteine mutants of Tim10 suggested that the mutants had impaired folding and displayed reduced solubility and stability, relative to the wild-type protein.[13]

Previous *in vitro* studies have employed radiolabeled cysteine mutants of Tim9 and Tim10 to dissect the residues required for docking onto Mia40 and subsequent release. It was shown that docking onto Mia40 strictly depends on the first cysteine in both Tim9 and Tim10. However, mutation of any of the remaining cysteine residues (C2, C3, C4) did not impair the interaction with Mia40 but rather perturbed oxidation and subsequent assembly.[20,21] Surprisingly, our *in vivo* results showed that yeast cells can overcome the hurdle of not having these cysteine residues and manage to import these proteins into mitochondria. This was even the case with loss of the first cysteine in Tim9 or Tim10, which showed profound effects when analyzed *in vitro*;[20,21] however, we could show that Tim10^{C40S} has the capacity to assemble as efficiently as wild-type Tim10 *in vivo*. Previously, it was shown that Mia40 recognizes a MISS/ITS signal adjacent to the most N-terminal cysteine residue of Tim9–Tim10.[33,34] It is possible that this signal can still be recognized by Mia40 even without the cysteine residue, thereby providing sufficient driving force for precursor entry into mitochondria. Our results led us to question the reason for discrepancies with the previous *in vitro* studies. Previously, the *in vitro* analysis focused on using radiolabeled mutant small TIM proteins and importing them into wild-type mitochondria. Since these mitochondria contain endogenous wild-type protein, we suggest that the imported mutants cannot effectively compete for assembly. It is also likely that the maturation pathway is also slowed. In this study, we removed the wild-type subunit from cells and this has allowed us to demonstrate that the mutant version has the capacity to overcome the barriers imposed within an *in vitro* situation and function within mitochondria in a cellular context.

The inability of the inner disulfide mutants to assemble into the hexameric complex seems to render the monomeric mutant protein and the respective wild-type partner protein unstable. This would suggest that these proteins are labile as individual entities within the IMS, and this mechanism would represent an efficient process to regulate the turnover of excess, unassembled subunits within the organelle. This phenomenon has also been observed in the case of Tim8 and Tim13, where the lack of one partner protein results in the loss of another partner at the steady-state level.[35,36] The reduced steady-state levels of the double-cysteine mutants and some of the single-cysteine mutants and the respective partner proteins hinted towards instability due to improper folding, leading to proteolytic turnover within mitochondria. Upon removal of the *i*-AAA protease component Yme1, we could restore the steady-state levels of mutant Tim9 in addition to the wild-type partner protein Tim10.

Furthermore, we observed accumulation of the proteins in cells bearing an inactive variant Yme1^{E541Q}, suggesting direct regulation of the mutant and unassembled small TIM levels by Yme1. The *i*-AAA protease is known to mediate proteolysis of unassembled and misfolded inner membrane proteins.[37] Recently, the first soluble IMS substrates for this molecular machine were described.[38] Based on our observations, we can now include misfolded and unassembled Tim9 and Tim10 as IMS substrates regulated by the *i*-AAA protease. Since only a handful of endogenous Yme1 substrates have been identified thus far in yeast, this study extends the substrate spectrum of this vital mitochondrial machine. It waits to be determined if the wild-type small TIM subunits are regulated by Yme1, or if another mechanism exists to regulate their levels.

In summary, this study provides novel insights into the fate of misfolded/unassembled proteins of the mitochondrial IMS. Using the classical MIA substrates, the small TIMs, we have shown that their inability to fold and consequently assemble due to incomplete oxidation results in the proteolytic clearance of these proteins from mitochondria. It is important to note that mutation of the fourth cysteine in the human Tim8 ortholog, DDP1 (deafness dystonia peptide 1), has been linked to the neurodegenerative disorder Mohr–Tranebjaerg syndrome.[39] Specifically, the DDP1^{C66W} mutant can no longer assemble with its partner protein, Tim13; thus, an assembly defect is the molecular basis for this disease. Our data are in agreement with these observations and such *in vivo* analyses are crucial in order for us to gain a true insight into the mechanisms governing protein oxidation and protein homeostasis in mitochondria.

Experimental Procedures

Cloning and construction of yeast strains

Yeast Tim9 and Tim10, including endogenous promoter and terminator regions, were cloned into the centromeric plasmids pRS415 (*LEU2*) and pRS413 (*HIS3*), respectively. Mutations were introduced by using overlap polymerase chain reaction using Pfusion™. The desired plasmids were transformed into *tim9*Δ (GB090) cells for Tim9 mutants or *tim10*Δ (GB100) cells for Tim10 mutants. Transformants were passaged on minimal SD medium (+glucose) supplemented with 650 mg/L of 5-FOA (SciMaR) and grown at 24 °C for loss of plasmids containing the *URA3* gene and wild-type Tim9 or Tim10. Viable strains were subjected to two passages on 5-FOA-containing media and subsequently passaged on YPG to assess growth on a non-fermentable carbon source. For generation of *tim9*$^{C39S/C55S}$/*yme1*Δ or *tim10*$^{C44S/C61S}$/*yme1*Δ, the complete *YME1* open reading frame was disrupted in *tim9*$^{C39S/C55S}$ cells by homologous recombination using the nourseothricin (NAT) cassette. For complementation analysis, the *tim9*$^{C39S/C55S}$/*yme1*Δ cells were transformed with plasmids encoding wild-type Yme1 (pRS314-Yme1^{WT}) or an inactive variant Yme1^{E541Q} (pRS316-Yme1^{E541Q}).

Preparation of yeast whole-cell extracts

Yeast whole-cell extracts were isolated according to previously published procedures.[40] Briefly, 10 mg of yeast cells was lysed by the addition of 0.3 M NaOH and 7.4% 2-mercaptoethanol and incubated on ice for 10 min. Protein was precipitated by trichloroacetic acid (TCA) for 10 min on ice. Samples were centrifuged for 2 min at maximum speed in a bench top refrigerated centrifuge. The resulting pellets were washed with ice-cold acetone and proteins were solubilized in Laemmli buffer at 95 °C for 5 min with vigorous shaking.

Mitochondrial *in vitro* import assays

Mitochondria were isolated by differential centrifugation and stored in SEM buffer (250 mM sucrose, 1 mM ethylenediaminetetraacetic acid, and 10 mM Mops–KOH, pH 7.2) at −80 °C.[41] Radiolabeled precursor proteins were generated by *in vitro* transcription/translation in the presence of [^{35}S]methionine/cysteine using rabbit reticulocyte lysate (Promega).[41] Mitochondria were added to import buffer [3% (w/v) fatty acid-free bovine serum albumin, 250 mM sucrose, 80 mM KCl, 5 mM $MgCl_2$, 5 mM methionine, 2 mM KH_2PO_4, and 10 mM Mops–KOH, pH 7.2] supplemented with an energy-regenerating system (4 mM ATP, 2 mM NADH, 100 µg/µl creatine kinase, and 5 mM creatine phosphate) and preincubated at 25 °C or 30 °C for 2 min. The import was initiated by the addition of precursor containing reticulocyte lysate [5–10% (v/v) of import reaction]. After the indicated times, mitochondria were isolated by centrifugation and washed in SEM buffer. Samples to be analyzed by Tris–*N*-[2-hydroxy-1,1-bis(hydroxymethyl)ethyl]glycine polyacrylamide gel electrophoresis were solubilized in Laemmli buffer.

Mitochondrial solubilization assay

Mitochondria isolated from wild-type and *tim9*$^{C39S/C55S}$/*yme1*Δ yeast cells were solubilized at 1 mg/ml in solubilization buffer {20 mM 2-[bis(2-hydroxyethyl)amino]-2-(hydroxymethyl)propane-1,3-diol, pH 7,4, 0.1 mM ethylenediaminetetraacetic acid, 50 mM NaCl, and 10% (w/v) glycerol} supplemented with 0.5%, 1%, or 1.5% digitonin or Triton X-100 and complete protease inhibitor cocktail (Roche). Mitochondria were solubilized on ice for 30 min and subsequently centrifuged at 21,000*g* for 30 min at 4 °C. Solubilized material was transferred to a new tube, and the soluble supernatant and insoluble pellet fractions were precipitated with 12.5% TCA.

Blue native polyacrylamide gel electrophoresis

Mitochondrial pellets (50 µg of protein) were resuspended in 45 µl of ice-cold solubilization buffer containing 1% digitonin and were incubated on ice for 10–15 min.

Samples were clarified by centrifugation at 12,000*g* for 15 min at 4 °C, and 5 µl of sample buffer {5% (w/v) Coomassie brilliant blue G-250, 100 mM 2-[bis(2-hydroxyethyl)amino]-2-(hydroxymethyl)propane-1,3-diol, pH 7.0, and 500 mM ε-amino-*n*-carponic acid} was added to the clarified supernatant. Samples were separated on a 4–16% polyacrylamide gradient gel at 4 °C, and the radiolabeled proteins were detected by digital autoradiography.

Acknowledgements

We thank Alexander Lowdin for technical assistance and Prof. Nikolaus Pfanner for generously providing us with antibodies. This work is supported by the Australian Research Council. D.S. is supported by an Australian Post-Doctoral Fellowship and a European Molecular Biology Organisation Short-Term Fellowship.

Received 17 July 2012;
Received in revised form 14 September 2012;
Accepted 17 September 2012
Available online 2 October 2012

Keywords:
disulfide bond;
intermembrane space;
MIA;
mitochondria;
Yme1

Abbreviations used:
TOM, translocase of the outer membrane; TIM, translocase of the inner membrane; IMS, intermembrane space; MIA, mitochondrial IMS import and assembly machinery; AAA, ATPases associated with diverse cellular activities; BN-PAGE, blue native polyacrylamide gel electrophoresis; Yme1, yeast mitochondrial escape 1; 5-FOA, 5-fluoroorotic acid; AAC, ADP/ATP carrier; DHFR, dihydrofolate reductase; SAM, sorting and assembly machiner; TCA, trichloroacetic acid; *i*-AAA, *IMS*-AAA.

References

1. Dolezal, P., Likic, V., Tachezy, J. & Lithgow, T. (2006). Evolution of the molecular machines for protein import into mitochondria. *Science*, **313**, 314–318.
2. Chacinska, A., Koehler, C. M., Milenkovic, D., Lithgow, T. & Pfanner, N. (2009). Importing mitochondrial proteins: machineries and mechanisms. *Cell*, **138**, 628–644.
3. Neupert, W. & Herrmann, J. M. (2007). Translocation of proteins into mitochondria. *Annu. Rev. Biochem.* **76**, 723–749.
4. Bolender, N., Sickmann, A., Wagner, R., Meisinger, C. & Pfanner, N. (2008). Multiple pathways for sorting mitochondrial precursor proteins. *EMBO Rep.* **9**, 42–49.
5. Stojanovski, D., Müller, J. M., Milenkovic, D., Guiard, B., Pfanner, N. & Chacinska, A. (2008). The MIA system for protein import into the mitochondrial intermembrane space. *Biochim. Biophys. Acta*, **1783**, 610–617.
6. Baker, M. J., Frazier, A. E., Gulbis, J. M. & Ryan, M. T. (2007). Mitochondrial protein-import machinery: correlating structure with function. *Trends Cell Biol.* **17**, 456–464.
7. Koehler, C. M. (2004). New developments in mitochondrial assembly. *Annu. Rev. Cell Dev. Biol.* **20**, 309–335.
8. Webb, C. T., Gorman, M. A., Lazarou, M., Ryan, M. T. & Gulbis, J. M. (2006). Crystal structure of the mitochondrial chaperone TIM9.10 reveals a six-bladed alpha-propeller. *Mol. Cell*, **21**, 123–133.
9. Baker, M. J., Webb, C. T., Stroud, D. A., Palmer, C. S., Frazier, A. E., Guiard, B. *et al.* (2009). Structural and functional requirements for activity of the Tim9–Tim10 complex in mitochondrial protein import. *Mol. Biol. Cell*, **20**, 769–779.
10. Beverly, K. N., Sawaya, M. R., Schmid, E. & Koehler, C. M. (2008). The Tim8–Tim13 complex has multiple substrate binding sites and binds cooperatively to Tim23. *J. Mol. Biol.* **382**, 1144–1156.
11. Koehler, C. M., Jarosch, E., Tokatlidis, K., Schmid, K., Schweyen, R. J. & Schatz, G. (1998). Import of mitochondrial carriers mediated by essential proteins of the intermembrane space. *Science*, **279**, 369–373.
12. Sirrenberg, C., Bauer, M. F., Guiard, B., Neupert, W. & Brunner, M. (1996). Import of carrier proteins into the mitochondrial inner membrane mediated by Tim22. *Nature*, **384**, 582–585.
13. Allen, S., Lu, H., Thornton, D. & Tokatlidis, K. (2003). Juxtaposition of the two distal CX3C motifs via intrachain disulfide bonding is essential for the folding of Tim10. *J. Biol. Chem.* **278**, 38505–38513.
14. Stojanovski, D., Bragoszewski, P. & Chacinska, A. (2012). The MIA pathway: a tight bond between protein transport and oxidative folding in mitochondria. *Biochim. Biophys. Acta*, **1823**, 1142–1150.
15. Herrmann, J. M. & Riemer, J. (2011). The mitochondrial disulfide relay: redox-regulated protein import into the intermembrane space. *J. Biol. Chem.* **287**, 4426–4433.
16. Hell, K. (2008). The Erv1-Mia40 disulfide relay system in the intermembrane space of mitochondria. *Biochim. Biophys. Acta*, **1783**, 601–609.
17. Chacinska, A., Pfannschmidt, S., Wiedemann, N., Kozjak, V., Sanjuán Szklarz, L. K., Schulze-Specking, A. *et al.* (2004). Essential role of Mia40 in import and assembly of mitochondrial intermembrane space proteins. *EMBO J.* **23**, 3735–3746.
18. Mesecke, N., Terziyska, N., Kozany, C., Baumann, F., Neupert, W., Hell, K. & Herrmann, J. M. (2005). A disulfide relay system in the intermembrane space of mitochondria that mediates protein import. *Cell*, **121**, 1059–1069.
19. Naoé, M., Ohwa, Y., Ishikawa, D., Ohshima, C., Nishikawa, S., Yamamoto, H. & Endo, T. (2004). Identification of Tim40 that mediates protein sorting to the mitochondrial intermembrane space. *J. Biol. Chem.* **279**, 47815–47821.

20. Milenkovic, D., Gabriel, K., Guiard, B., Schulze-Specking, A., Pfanner, N. & Chacinska, A. (2007). Biogenesis of the essential Tim9–Tim10 chaperone complex of mitochondria: site-specific recognition of cysteine residues by the intermembrane space receptor Mia40. *J. Biol. Chem.* **282**, 22472–22480.
21. Sideris, D. P. & Tokatlidis, K. (2007). Oxidative folding of small Tims is mediated by site-specific docking onto Mia40 in the mitochondrial intermembrane space. *Mol. Microbiol.* **65**, 1360–1373.
22. Ryan, M. T., Müller, H. & Pfanner, N. (1999). Functional staging of ADP/ATP carrier translocation across the outer mitochondrial membrane. *J. Biol. Chem.* **274**, 20619–20627.
23. Wiedemann, N., Pfanner, N. & Ryan, M. T. (2001). The three modules of ADP/ATP carrier cooperate in receptor recruitment and translocation into mitochondria. *EMBO J.* **20**, 951–960.
24. Hoppins, S. C. & Nargang, F. E. (2004). The Tim8–Tim13 complex of *Neurospora crassa* functions in the assembly of proteins into both mitochondrial membranes. *J. Biol. Chem.* **279**, 12396–12405.
25. Wiedemann, N., Truscott, K. N., Pfannschmidt, S., Guiard, B., Meisinger, C. & Pfanner, N. (2004). Biogenesis of the protein import channel Tom40 of the mitochondrial outer membrane: intermembrane space components are involved in an early stage of the assembly pathway. *J. Biol. Chem.* **279**, 18188–18194.
26. Model, K., Meisinger, C., Prinz, T., Wiedemann, N., Truscott, K. N., Pfanner, N. & Ryan, M. T. (2001). Multistep assembly of the protein import channel of the mitochondrial outer membrane. *Nat. Struct. Biol.* **8**, 361–370.
27. Wiedemann, N., Kozjak, V., Chacinska, A., Schönfisch, B., Rospert, S., Ryan, M. T. *et al.* (2003). Machinery for protein sorting and assembly in the mitochondrial outer membrane. *Nature*, **424**, 565–571.
28. Koppen, M. & Langer, T. (2007). Protein degradation within mitochondria: versatile activities of AAA proteases and other peptidases. *Crit. Rev. Biochem. Mol. Biol.* **42**, 221–242.
29. Baker, M. J., Tatsuta, T. & Langer, T. (2011). Quality control of mitochondrial proteostasis. *Cold Spring Harbor Perspect. Biol.* **3**.
30. Tatsuta, T. & Langer, T. (2009). AAA proteases in mitochondria: diverse functions of membrane-bound proteolytic machines. *Res. Microbiol.* **160**, 711–717.
31. Truscott, K. N., Lowth, B. R., Strack, P. R. & Dougan, D. A. (2010). Diverse functions of mitochondrial AAA+ proteins: protein activation, disaggregation, and degradation. *Biochem. Cell Biol.* **88**, 97–108.
32. Leonhard, K., Stiegler, A., Neupert, W. & Langer, T. (1999). Chaperone-like activity of the AAA domain of the yeast Yme1 AAA protease. *Nature*, **398**, 348–351.
33. Milenkovic, D., Ramming, T., Müller, J. M., Wenz, L. S., Gebert, N., Schulze- Specking, A. *et al.* (2009). Identification of the signal directing Tim9 and Tim10 into the intermembrane space of mitochondria. *Mol. Biol. Cell*, **20**, 2530–2539.
34. Sideris, D. P., Petrakis, N., Katrakili, N., Mikropoulou, D., Gallo, A., Ciofi-Baffoni, S. *et al.* (2009). A novel intermembrane space-targeting signal docks cysteines onto Mia40 during mitochondrial oxidative folding. *J. Cell Biol.* **187**, 1007–1022.
35. Müller, J. M., Milenkovic, D., Guiard, B., Pfanner, N. & Chacinska, A. (2008). Precursor oxidation by Mia40 and Erv1 promotes vectorial transport of proteins into the mitochondrial intermembrane space. *Mol. Biol. Cell*, **19**, 226–236.
36. Koehler, C. M., Leuenberger, D., Merchant, S., Renold, A., Junne, T. & Schatz, G. (1999). Human deafness dystonia syndrome is a mitochondrial disease. *Proc. Natl Acad. Sci. USA*, **96**, 2141–2146.
37. Leonhard, K., Guiard, B., Pellecchia, G., Tzagoloff, A., Neupert, W. & Langer, T. (2000). Membrane protein degradation by AAA proteases in mitochondria: extraction of substrates from either membrane surface. *Mol. Cell*, **5**, 629–638.
38. Potting, C., Wilmes, C., Engmann, T., Osman, C. & Langer, T. (2010). Regulation of mitochondrial phospholipids by Ups1/PRELI-like proteins depends on proteolysis and Mdm35. *EMBO J.* **29**, 2888–2898.
39. Tranebjaerg, L., Hamel, B. C., Gabreels, F. J., Renier, W. O. & Van Ghelue, M. (2000). A de novo missense mutation in a critical domain of the X-linked DDP gene causes the typical deafness–dystonia–optic atrophy syndrome. *Eur. J. Hum. Genet.* **8**, 464–467.
40. Yaffe, M. P. & Schatz, G. (1984). Two nuclear mutations that block mitochondrial protein import in yeast. *Proc. Natl Acad. Sci. USA*, **81**, 4819–4823.
41. Stojanovski, D., Pfanner, N. & Wiedemann, N. (2007). Import of proteins into mitochondria. *Methods Cell Biol.* **80**, 783–806.